Multi-port excitation at high field MRI: Trade-off between B1+ homogeneity and RF heating

C. A. van den Berg[1], J. B. van de Kamer[1], H. P. Kok[2], J. J. Lagendijk[1], L. W. Bartels[3]

[1]Department of Radiotherapy, University Medical Center Utrecht, Utrecht, Utrecht, Netherlands, [2]Department of Radiation Oncology, Academic Medical Centre University of Amsterdam, Amsterdam, Netherlands, [3]Department of Radiology, Image Sciences Institute, University Medical Center Utrecht, Utrecht, Utrecht, Netherlands

Introduction:

Various numerical studies have shown that for high field MR (> 3 Tesla) the B_1^+ excitation field is heterogeneous due to the finite RF wavelength inside the human body [1,2]. Dielectric resonance and RF penetration effects causing severe degradation of the image quality have been reported both numerically and experimentally. Furthermore, the high dielectric contrast in the human body can lead to local high SAR values [3]. This concern has become more acute at high field MR imaging since the RF dissipation increases with the square of the RF frequency. Attempts to verify whether SAR hotspots correlate to actual temperature rise have been limited. To overcome the problem of B_1^+ inhomogeneity the concept of multi-port excitation has been proposed and it was shown that local B_1^+ homogeneity can be improved significantly [4]. The impact of phase/amplitude modulation on the SAR distribution has gained less attention, although the need for an extensive safety analysis was demonstrated [5]. In this study we numerically investigated the potential of multi-port excitation at 7 Tesla for improving local B_1^+ homogeneity. Unique in our approach is the inclusion of the temperature as a constraint into the actual optimization process. By looking directly at the temperature rise instead of SAR for a given phase/amplitude setting, it is expected that the potential of multi-port excitation can be better exploited. Peak SAR values are assessed on their actual temperature rise, which is supposed to form a less constraining factor.

Materials and Methods:

For this study we modeled a RF transit system operating at 298 MHz by defining six independent electrical dipole antennas consisting of copper rods, which were surrounded by a RF shield. In the center a cylindrical phantom was placed (length 65 cm, ∅21 cm). The dielectric properties were chosen analog to muscle at 298 MHz/ 7T (table 1). Separate FDTD simulations were done of the field distributions of each antenna at an isotropic resolution of 5 mm. Calculation of the resulting B_1^+ distribution was performed by superposition of the transverse magnetic field component B_x and B_y of each antenna in an optimization process in which the phase and amplitude of the antennas was varied freely. The objective of the optimization was to minimize the standard deviation of the $|B_1^+|$ in a certain arbitrarily defined region in the phantom. See figure 1. For all simulations the $|B_1^+|$ field was normalized at an average value of 6 μT in the region of interest, which corresponds to a 90 degree pulse for a 1 ms RF pulse duration. A duty cycle τ_{rf}/ Tr of 10 % and a scan time of 3 minutes was assumed.

	Dielectric Constant	Electrical Conductivity (S/m)	Thermal Conductivity (W/m/K)	Perfusion (ml/100gr/min)
Phantom	60	0.8	0.6	21
ROI	60	0.8	0.6	21
Copper	1	$5.8 \cdot 10^7$	390	0
Air	1	0	0.02	0

Table 1: Dielectric and Thermal properties

The temperature constraint was implemented inherently in the optimization process. The temperature elevation was calculated by numerically solving the Pennes bio-heat equation using a complex formulation of the temperature[6]. In this way the temperature elevation can be computed during the optimization process for any phase/amplitude settings without having to solve the Pennes bio-heat equation again. As a constraint a maximum temperature rise of could be set. The initial phantom and ambient temperatures were set at 37 °C and 20 °C respectively.

Results:

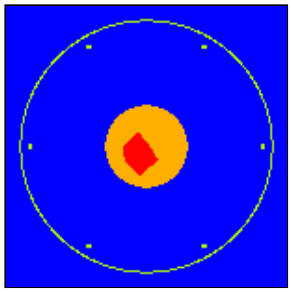

Fig.1: Transverse overview of geometry. The cylinder is surrounded by antennas (length 56 cm) and the RF shield (length 80 cm, ∅ 66 cm). Inside the cylinder an arbitrarily region-of-interest is drawn.

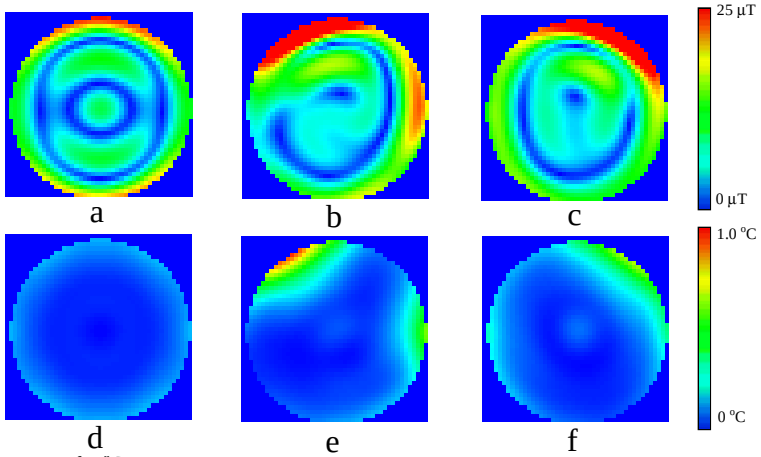

Fig 2. $|B_1^+|$ and temp. distribution for different P/A settings in transverse plane at location of region of interest:
a:) $|B_1^+|$ "birdcage" settings. Note the "dielectric resonance" effect
b:) $|B_1^+|$ optimized P/A settings with 1 °C temp. rise constraint.
c:) $|B_1^+|$ optimized P/A setting with 0.6 °C temp. rise constraint.
d - f:) Corresponding temperature after 3 min. of scanning.

Table 2 shows that with a temperature rise constraint of 1 °C an improvement of a factor 2.5 in local B_1^+ homogeneity could be achieved in comparison with standard "birdcage" settings. The results for a temperature rise constraint of 0.6 °C show that simultaneous reduction in RF heating and improvement of local B_1^+ homogeneity is possible.

	Average B_1^+ (μT) in region of interest	Standard Deviation B_1^+ in region of interest (% of average)	Average SAR in phantom (W/kg)	Average Temp. rise in phantom (°C)	Maximum Temp. Rise in phantom (°C)
Birdcage Settings	6	53	4.8	0.18	0.68
P/A settings (ΔT = 1.0 °C)	6	20	5	0.18	0.96
P/A settings (ΔT = 0.6 °C)	6	33	3.6	0.12	0.59

Table 2: Overview of results.

Conclusions:

It was shown that for high field MR the temperature elevation due to RF heating is considerable. The presented method allows assessment of multi-port excitation in terms of local B_1^+ homogeneity and limitation of RF heating simultaneously. Since the performance of multi-port excitation is determined by the trade off betweens these two aspects, it is thought that the presented method will be a valuable tool. This method may also be used to limit the RF heating during "RF-intensive" sequences by minimizing the local or global temperature elevation with multi-port excitation. In the near future the method will be extended towards human anatomies.

References: 1: T.S. Ibrahim et al. Proc. ISMRM 2004, 2: DeMeester et al. Proc. ISMRM 2004, 3: Van de Kamer et al. Int J Hyperthermia. 18 (2) 2002 , 4: Ibrahim et al, Magn. Reson. Imag 19 2001. 5: Wuebbeler et al, Proc. ISMRM 2004, 6: Das et al, Med. Phys 26(2) 1999.